Open Access

Advances in Environmental and Engineering Research

LIDSEN Publishing Inc.

Original Research

Assessing Land Use Dynamics and Thermal Stress in Ahmedabad Using Integrated Remote Sensing and Machine Learning Techniques

Rupesh Kumar Gupta [1], Yash Kumar Tiwari [1], Arpit Gupta [1], Grinedge Yadav [1], Swati Gupta [2, *]

1. Department of Continuing Education and Extension, Faculty of Social Sciences, University of Delhi, Delhi-110007, India; E-Mails: gisrs2004@gmail.com; phd.yash0402@gmail.com; arpitgupta2662@gmail.com; grinedge.du@gmail.com
2. Central Board of Secondary Education, New Delhi, India; E-Mail: drswatigupta1205@gmail.com

* **Correspondence:** Swati Gupta; E-Mail: drswatigupta1205@gmail.com

Academic Editor: Amin Beiranvand Pour

Adv Environ Eng Res
2026, volume 7, issue 2
doi:10.21926/aeer.2602011

Received: March 01, 2026
Accepted: May 14, 2026
Published: May 27, 2026

Abstract

The rapid urbanisation in developing countries has not only intensified land transformation but also significantly altered surface temperatures, thereby increasing climate vulnerability. Ahmedabad, one of India's fastest-growing cities, has witnessed substantial urban growth over the past two decades and therefore requires an integrated approach to analyse land-use change, thermal dynamics, and future growth patterns. This study aims to analyse the spatial and temporal patterns of land use/land cover (LULC) changes, examine their association with land surface temperature (LST) and urban thermal stress, and simulate future LULC patterns for the year 2045. Multi-temporal Landsat imagery from 2000 and 2020 was used to map LULC using a Random Forest classifier implemented on the Google Earth Engine platform, achieving an overall classification accuracy of approximately 89-93%. Urban thermal conditions were assessed using MODIS-derived LST data, and thermal stress was evaluated using the Urban Thermal Field Variance Index (UTFVI). The results indicate that built-up areas expanded from approximately 161 km^2 in 2000 to 223 km^2 in 2020, primarily due to the conversion of barren land, vegetation, and agricultural areas. LST patterns revealed a significant intensification of high-temperature zones, particularly in densely built-up and industrial regions. The UTFVI

analysis shows that more than 60% of the city experiences moderate to high thermal stress, while areas with higher vegetation cover and water bodies consistently exhibit lower thermal stress. Future simulations suggest that built-up areas may exceed 300 km^2 by 2045, further intensifying urban heat stress if current land-use trends continue. The integrated LULC-LST-UTFVI framework highlights the critical role of land-use planning in developing climate-responsive urban strategies and mitigating thermal stress in rapidly expanding cities.

Keywords
Land use/land cover; urban heat stress; urban microclimate; predictive modelling; GIS

1. Introduction

Land Use and Land Cover (LULC) are generally understood as two closely related but conceptually different components of the surface of the earth. At the same time, land use refers to the functional, social and economic utilization of land. In contrast, land cover represents the observable natural features of the Earth's surface, including croplands, water bodies, forests, and built-up areas [1]. In various classification schemes, these categories often appear discrete; however, in rapidly growing urban areas, they are highly dynamic. The changes in LULC, mostly driven by human activities, are not merely superficial; they alter ecosystem processes, hydrological regimes, and local microclimate [2], particularly in cities with very high growth rates. The important task is understanding how these patterns are shifting over time and how those shifts affect the environment's stability. In this context, LULC analysis plays a vital role within land-use planning frameworks [3, 4] by assessing LULC transitions to help planners predict future expansion trends and evaluate the pressure that may be placed on natural and socio-ecological resources [5]. In a rapidly growing metropolitan region like Ahmedabad, where infrastructure growth and urban expansion have extended outward from the city into peri-urban zones, examining LULC change trends is essential to balance development plans with environmental constraints and support more effective climate-responsive planning strategies.

Human modification of the land has contributed to higher agricultural productivity, infrastructure expansion, and improved standards of living [6], but the current phase of LULC change differs markedly from earlier periods in both scale and intensity. Recent global studies show that more than 50 percent of Earth's surface exhibits measurable indications of human influence on LULC [6, 7]. Such large-scale modifications are not environmentally neutral, as alterations in LULC influence surface runoff patterns, ecological habitats, and the surface-atmosphere energy balance [8, 9], especially in areas of high stress on natural resources. While rapid population growth and unregulated urban expansion are often cited as important causes of LULC change [10, 11], these processes do not operate in isolation, as their impacts are shaped by policies, regulations, governance, and existing environmental conditions [12-15].

Geospatial technologies, including remote sensing and GIS, are very important for monitoring LULC, as they can produce consistent, multi-temporal datasets across large geographic areas [16]. In recent times, the integration of machine learning has improved the efficiency and reliability of LULC classification using techniques such as Random Forest, Support Vector Machines, and ANNs

across diverse urban environments [17, 18]. Beyond mapping, these predictive modelling approaches increase the scope of analysis by simulating possible future scenarios [19, 20].

In the rapidly urbanizing city of Ahmedabad, significant LULC transformations have been visible over the last few decades. These changes have been characterised by continuous outward growth of human-constructed areas and the loss of vegetation and agricultural land [21, 22]. As a result, there is an increase in pressure on natural resources, particularly water availability and open spaces, and the physical characteristics of the land surface have shifted to impervious and heat-retaining materials like concrete, asphalt, etc. [23].

These changes in LULC, such as replacing permeable and vegetated surfaces with concrete and asphalt, significantly influence the urban microclimate by altering the surface energy balance, reducing evapotranspiration, and contributing to rising land surface temperatures. Such changing patterns are closely linked to the intensification of the Urban Heat Island (UHI) effect, especially in major Indian cities [24-29]. In this context, it is not sufficient to assess LULC changes and thermal characteristics in isolation; an integrated framework is needed that systematically analyses LULC transitions in relation to environmental and climatic responses. Such an approach helps to get a more comprehensive overview of urban growth impacts and provides a stronger basis for climate-responsive and sustainable urban planning strategies [26-30].

A substantial body of literature has studied LULC dynamics in both Indian and international contexts, showing rapid expansion of built-up areas and associated environmental impacts. In the Indian context, Sudhira et al. [18] highlighted that accelerated urban growth in Bangalore has led to the fragmentation of UGS and increased landscape heterogeneity. Similar trends have also been studied in Ajmer [31] and parts of Uttarakhand [32], where rapid urban expansion has altered land-use patterns and exerted pressure on ecological systems. At the global level, Seto et al. [33] projected continued urban expansion across Asia and Africa, which raises significant environmental concerns like deforestation, habitat loss, and desertification. On the other hand, studies from Europe have reported a steady decline in vegetation cover, resulting in a measurable increase in land surface temperatures [34]. Similarly, Zhou et al. [35] showed that the land conversion from agricultural to built-up in rapidly developing Chinese cities has intensified the UHI effect. A few studies have also attempted to analyse thermal Stress and LULC dynamics, such as Mohan et al. [36], who found that in Delhi, dense commercial urban areas exhibit extremely high UHI intensities (up to 10.7°C), while forested zones like the Delhi Ridge act as significant thermal buffers. Aqdas et al. [37] showed in Ghaziabad that LST strongly correlates positively with built-up indices (NDBI) and negatively with vegetation (NDVI), with industrial and bare land surfaces reaching temperatures up to 46.30°C. Mahata et al. [38] reported that in New Town Kolkata, rapid built-up growth (21.91% to 45.63%) significantly increased summer LST (29.18°C to 34.61°C). Kavathekar et al. [39] found that in the Mumbai Metropolitan Region, a 77.82% increase in built-up area and a 37.17% loss of vegetation led to consistent LST increases of 1.5-2.5°C per decade, with industrial zones as major hotspots.

While these studies have advanced understanding of land-use transformation and its environmental implications, few investigations have combined multi-temporal LULC assessment, urban thermal stress evaluation, and future land-use simulation within a unified analytical framework. This gap limits the ability to comprehensively interpret how past transitions, current thermal conditions, and projected growth trajectories interact in rapidly urbanizing regions. To address this identified research gap, this study adopts an integrated geospatial framework that

combines remote sensing and GIS-based spatial analysis with machine learning algorithms and the MOLUSCE (Modules for Land Use Change Evaluation) model. This approach is applied to examine historical LULC transitions, evaluate urban thermal stress through LST analysis and UTFVI, and simulate potential future land-use scenarios within the Ahmedabad Metropolitan Region. By linking past land transformations with present thermal conditions and projected growth patterns, the study moves beyond isolated assessments of urban expansion. It seeks to systematically analyse how changes in land cover influence spatial patterns of thermal stress and how future development trajectories may further reshape the urban microclimate. Through this integrated LULC-LST-UTFVI modelling framework, this study aims to (i) quantify spatial-temporal LULC changes, (ii) examine their relationship with land surface temperature and thermal stress using UTFVI, and (iii) simulate future LULC scenarios using a CA-ANN model for Ahmedabad. The study aligns with the journal's requirements by integrating environmental monitoring with geospatial modelling to assess interactions between urban climate and its surrounding environment. The LULC-thermal coupling and predictive modelling give us valuable insights for environmental planning and engineering interventions aimed at climate-resilient urban systems.

2. Materials and Methods

2.1 Study Area

The Ahmedabad Metropolitan Region (AMR) is located in the western state of Gujarat, India, and is one of the rapidly growing urban centers of the country (Figure 1). Geographically, the region lies between 22°55′ and 23°08′ N latitude and 72°30′ and 72°42′ E longitude. Ahmedabad is influenced by semi-arid climatic conditions that feature hot summers, moderate monsoon rainfall, and moderate winters, making it particularly sensitive to land-use-induced thermal and environmental changes.

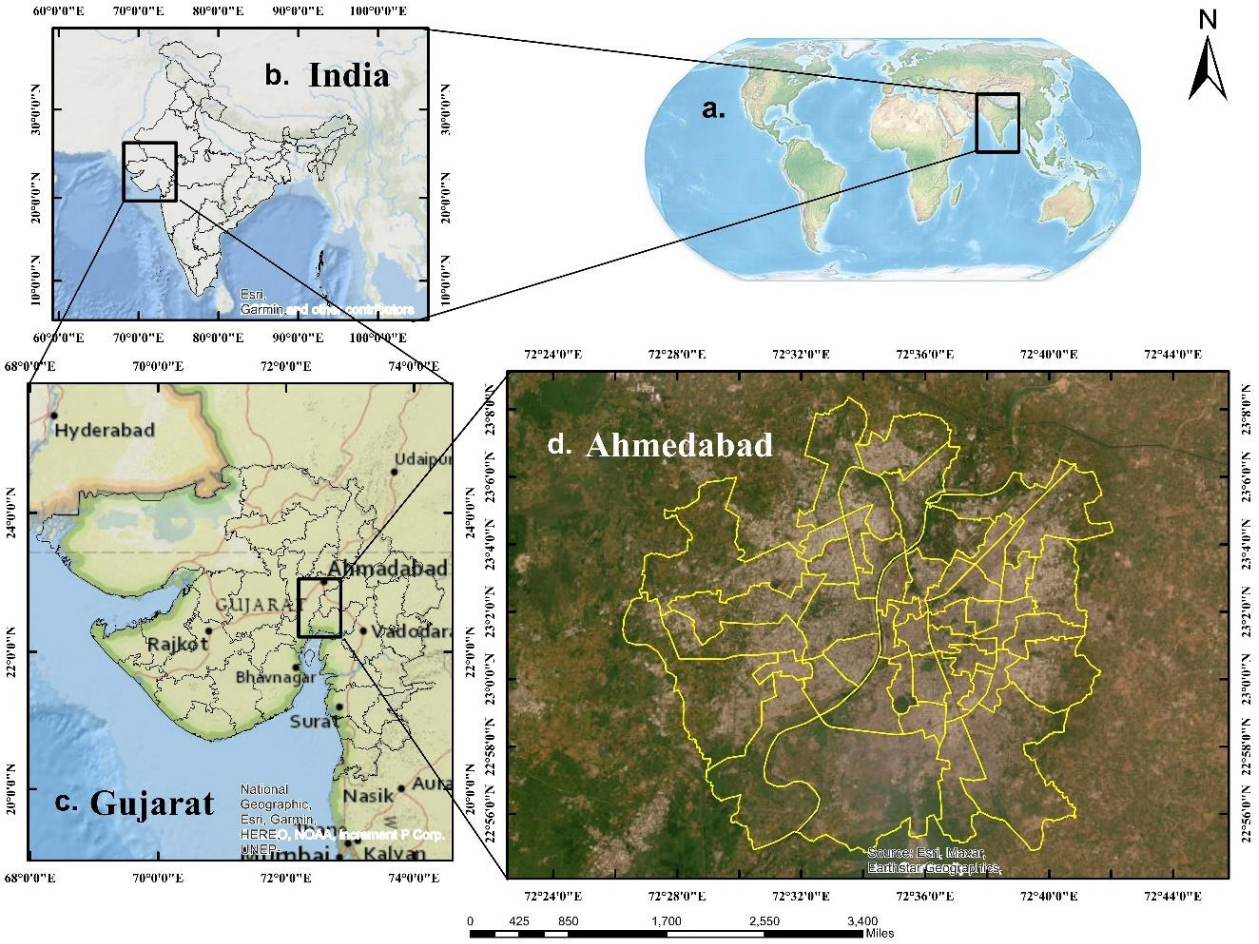

Figure 1 Study Area with (a) Location of the Indian Subcontinent in the world; (b) Location of India in the Indian Subcontinent; (c) Location of Gujarat; (d) Location of the Ahmedabad Metropolitan Region.

Ahmedabad has undergone significant expansion over the last 20 years, mainly driven by population growth, industrialisation, and large-scale infrastructure development. Between 2001 and 2011, the population grew from 3.52 million to 5.57 million, accompanied by outward urban sprawl and densification. This accelerated growth has exerted increasing pressure on land resources, vegetation cover, water bodies, and urban infrastructure, making Ahmedabad a suitable case for examining LULC dynamics, urban thermal stress, and predicting the upcoming growth trajectories.

2.2 Data Sources

The study utilizes multi-source satellite datasets with differing spatial resolutions, including Landsat imagery (30 m) for LULC classification and MODIS LST data (1 km) for thermal analysis. Each dataset was preprocessed independently according to its characteristics. Landsat imagery was radiometrically calibrated and classified at its native spatial resolution to preserve detailed land-cover information. MODIS LST data were processed to derive temperature values and subsequently resampled using bilinear interpolation to ensure spatial compatibility with the study framework. The analysis was conducted at an aggregated spatial scale to examine broader spatial relationships between land use patterns and thermal characteristics. This approach avoids scale-induced bias and is consistent with established practices in urban climate studies.

2.2.1 Satellite Data

This study employed multi-temporal satellite imagery to analyse land-use/land-cover change, land surface temperature, and urban thermal stress in Ahmedabad. Landsat imagery was used for detailed LULC mapping due to its moderate spatial resolution (30 m), which allows effective discrimination of urban and non-urban land cover types. Landsat 7 ETM+ imagery was utilized for the year 2000, while Landsat 8 OLI/TIRS imagery was used for 2020. All Landsat datasets were obtained from the USGS Collection 2 Tier 1 archive and calibrated to top-of-atmosphere (TOA) reflectance to ensure radiometric consistency for multi-temporal analysis [40, 41].

For thermal analysis, Moderate Resolution Imaging Spectroradiometer (MODIS) Land Surface Temperature (LST) products were used to assess spatial and temporal patterns of surface temperature. MODIS data provide long-term, consistent thermal observations at a 1 km spatial resolution, making them suitable for regional-scale urban thermal assessment. MODIS LST for June 2000 and 2020 was used as a representative peak summer condition to assess spatial patterns of urban thermal stress [26]. The integration of Landsat and MODIS datasets enabled the combined analysis of fine-scale land use changes and broader urban thermal dynamics. A summary of the satellite datasets used in this study is presented in Table 1.

Table 1 Satellite Datasets used.

S. No	Satellite	Spatial Resolution	Sensor	Time	Source
1	Landsat 7	30 m	ETM	June 2000	USGS Earth Explorer
2	Landsat 8	30 m	OLI & TIRS	June 2020	USGS Earth Explorer
3	MODIS	1 km	Terra	June 2000	NASA Earth Data

2.2.2 Auxiliary Spatial Data

To balance computational efficiency, several auxiliary spatial datasets were also used in the study to support land-use change modelling and future simulations. The Digital Elevation Model (DEM) was obtained from USGS Earth Explorer to derive terrain attributes for the study, including slope, aspect, curvature, hillshade, and contours. The hydrological data were obtained from the HydroSHEDS database to generate stream networks and distance-to-stream layers, whereas accessibility (roads and railways) was studied using transportation data taken from BBBike extracts by calculating proximity layers [42, 43].

These auxiliary variables represent both natural and human-made aspects of LULC changes and were integrated into the MOLUSCE modelling. The details of the auxiliary datasets used in the study are provided in Table 2.

Table 2 Spatial Variable Data and Specifications.

Data	Source	Acquisition Date	Utility
DEM	earthexplorer.usgs.gov/	01/03/2025	Slope Aspect Curvature Hill shade Contour
Stream	hydrosheds.org/	01/03/2025	Distance from Stream
Road	extract.bbbike.org/	01/03/2025	Distance from Road
Railway	extract.bbbike.org/	01/03/2025	Distance from Railway

Figure 2 shows the spatial distribution of the auxiliary variables used to model land use transitions in Ahmedabad. These variables represent both natural and anthropogenic drivers influencing urban growth. Terrain-related parameters, such as elevation, slope, and curvature, capture topographic constraints. At the same time, proximity-based variables, including distance to roads, railways, and streams, reflect accessibility and the influence of infrastructure on land conversion processes. These auxiliary variables were standardised in MOLUSCE to perform ANN-based simulations of future LULC patterns [41, 42].

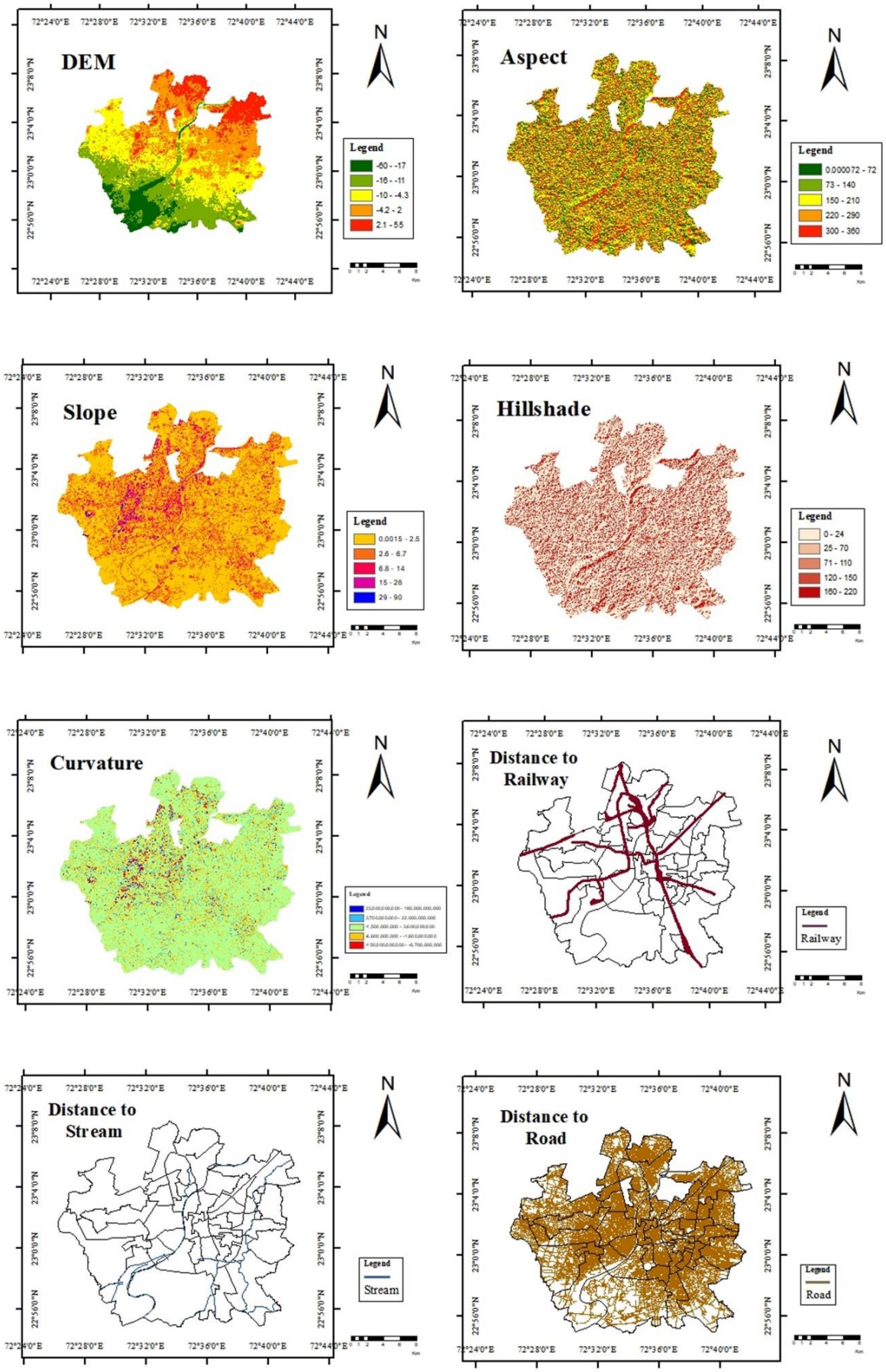

Figure 2 Spatial Distribution of Auxiliary Variables used for LULC Prediction.

2.3 Methods Used

2.3.1 LULC Classification

It was performed using a supervised technique, which was done by visually interpreting the satellite imagery and reference data [44-46]. For this, six major LULC classes were used, i.e., Built-up, Water Bodies, Dense Vegetation, Sparse Vegetation, Cropland, and Barren Land (Table 3). The training samples for each class used for classification were manually digitised using high-resolution reference imagery, i.e. Google Earth.

Table 3 Description LULC Classification Scheme.

LULC Type	Description	Training Sample Points
Built-up	Residential, Commercial, and Other Infrastructure	100
Water Body	Rivers, lakes, ponds, and dams	50
Dense Vegetation	All types of forest cover land	80
Sparse Vegetation	Parks, Green spaces, Wetland	80
Cropland	Agricultural Land, Farm Land, Fallow Land	80
Barren land	All types of barren land	50

For 2000, Landsat 7 ETM+ spectral bands (B1-B5 and B7) were used, while for 2020, Landsat 8 OLI bands (B2-B7) were selected to ensure optimal class separability.

2.3.2 Random Forest Classification

This scheme was used for LULC mapping because it is more robust to handling complex, heterogeneous urban features. The classifier was trained using labelled training samples, with 70% used for training and 30% reserved for validation. The RF model was run on the GEE platform because it is very capable of processing large amounts of satellite data at once [22, 23].

2.3.3 Accuracy Assessment

The accuracy of the maps for 2000 and 2020 was calculated using pixel-based accuracy assessment techniques. The confusion matrices were generated to calculate User's Accuracy, Producer's Accuracy, Overall Accuracy, and the Kappa Coefficient [47]. To validate the LULC classification, Google Earth images were taken as reference datasets. The classification accuracy obtained was analysed using a confusion matrix that was derived from the reference and classified data. For this, the standard accuracy formulae were used, which are listed as follows [47] (Equations 01-03):

Overall Accuracy (OA):

$$OA = \frac{\sum_{i=1}^{k} n_{ii}}{N} \times 100 \quad (1)$$

Producer's Accuracy (PA):

$$PA_i = \frac{n_{ii}}{\sum_{j=1}^{k} n_{ij}} \times 100 \quad (2)$$

User's Accuracy (UA):

$$UA_i = \frac{n_{ii}}{\sum_{j=1}^{k} n_{ji}} \times 100 \quad (3)$$

where:
n_{ii} = correctly classified pixels for class *i*
N = total number of reference pixels
k = number of classes

Kappa Coefficient (*κ*) was calculated to measure agreement beyond chance (Equation 4):

$$\kappa = \frac{N\sum n_{ii} - \sum(n_{i+}n_{+i})}{N^2 - \sum(n_{i+}n_{+i})} \quad (4)$$

2.3.4 LST and UTFVI Estimation

The LST was derived from MODIS Terra thermal satellite images to examine thermal patterns across Ahmedabad city [48-52]. The study integrates multi-source satellite datasets with differing spatial resolutions, namely Landsat (30 m) for LULC mapping and MODIS (1 km) for thermal analysis. To address this spatial resolution difference, the MODIS LST data were resampled to a finer spatial grid using bilinear interpolation. However, the analysis was conducted at an aggregated spatial level to ensure consistency between datasets. It is important to note that the objective is not pixel-level comparison, but rather to examine broader spatial relationships between land use patterns and urban thermal characteristics. The integration of Landsat and MODIS datasets thus provides complementary insights by combining detailed land cover information with consistent large-scale thermal observations.

The digital number values of the imagery were converted into temperature values using the following equation (Equation 5).

$$Temperature\ in\ °C = DN * 0.02 - 273.15 \quad (5)$$

where *DN* is the Digital Number of the MODIS LST product, for assessing the thermal stress zones of the city, the UTFVI was calculated using the following equation 6:

$$UTFVI = \frac{LST_i - LST_{mean}}{LST_{mean}} \quad (6)$$

LST_i = land surface temperature of pixel *i*
LST_{mean} = mean LST of the study area

The UTFVI values were further grouped into three thermal stress zones, i.e., high, medium, and low, in order to analyze the thermal stress patterns in intra-city conditions. UTFVI was selected as it normalizes LST relative to mean thermal conditions, enabling classification of ecological thermal stress zones, which is more informative than absolute temperature values for urban climate assessment.

2.3.5 Future Land Use Simulation Using MOLUSCE

The future LULC was simulated using MOLUSCE in QGIS, with classified LULC maps from 2000 and 2020 used as input layers for change detection and transition probability estimation [41, 42] (Figure 3). An ANN model was then trained using historical LULC and auxiliary variables as mentioned earlier. The ANN estimates the transition potential. P_{ij} between land use classes based on input driving factors using the following (Equation 7):

$$P_{ij} = f(\sum_{k=1}^{n} w_k \, x_k + b) \tag{7}$$

where:
x_k = driving variables (e.g., slope, distance to roads, streams)
w_k = weights associated with each variable
b = bias term
f = activation function

The model parameters, such as learning rate, number of hidden layers, number of iterations, and neighborhood size, were optimized to capture spatial transition patterns, and the trained ANN was then used to simulate LULC predictions for 2045 [41, 42]. The model performance was further evaluated using the Kappa Index of Agreement to assess how accurately the simulation was performed by the model, and the reliability of the predicted results using the Kappa Index of Agreement (KIA):

$$KIA = \frac{P_o - P_e}{1 - P_e} \tag{8}$$

where:
P_o = observed agreement
P_e = expected agreement by chance

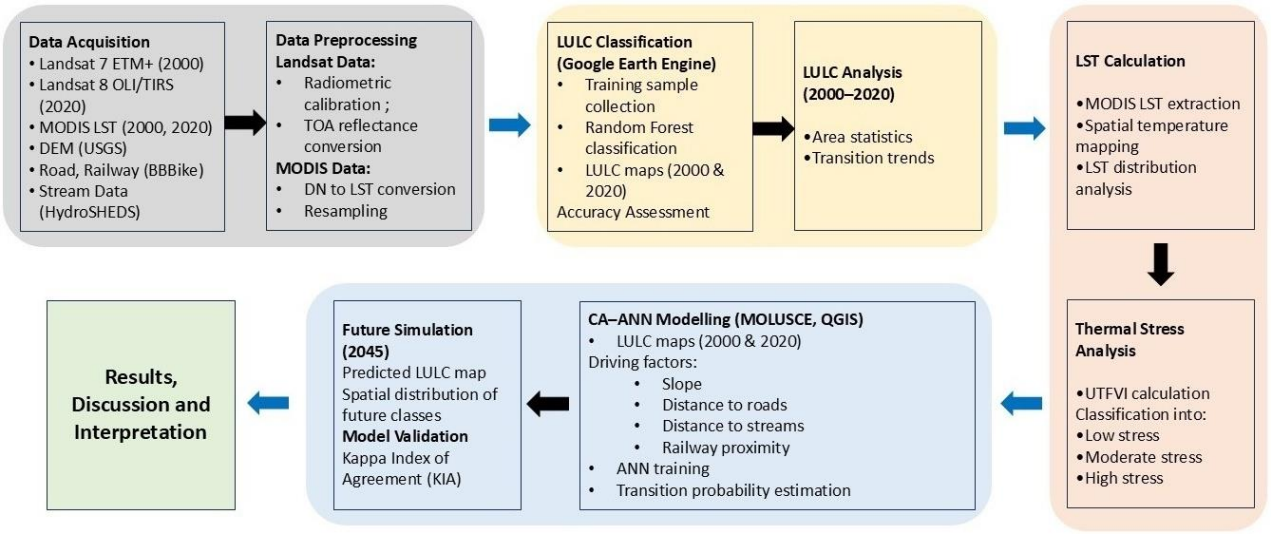

Figure 3 Flowchart of the Methodology used in the Study.

3. Results

3.1 Land Use and Land Cover Changes in Ahmedabad (2000-2020)

The LULC analysis of Ahmedabad reveals significant spatial transformations between 2000 and 2020, mainly driven by rapid urban expansion. The quantitative changes in LULC types for this period are listed in Table 4, while the maps indicating the spatial distribution of LULC for 2000 and 2020 are illustrated in Figure 4(a, b), respectively.

Table 4 LULC Area Statistics for Ahmedabad (2000 and 2020).

LULC Class	2000		2020		Change (2000-2020)	
	Area (km^2)	Per cent	Area (km^2)	Per cent	Area (km^2)	Per cent
Built-up	161.40	40.18%	223.39	55.60%	+61.99	+15.42%
Cropland	79.25	19.73%	97.35	24.23%	+18.10	+4.50%
Vegetation	33.04	8.22%	22.19	5.52%	-10.85	-2.70%
Barren Land	125.72	31.29%	50.84	12.65%	-74.88	-18.64%
Waterbody	2.33	0.58%	7.97	1.98%	+5.64	+1.40%

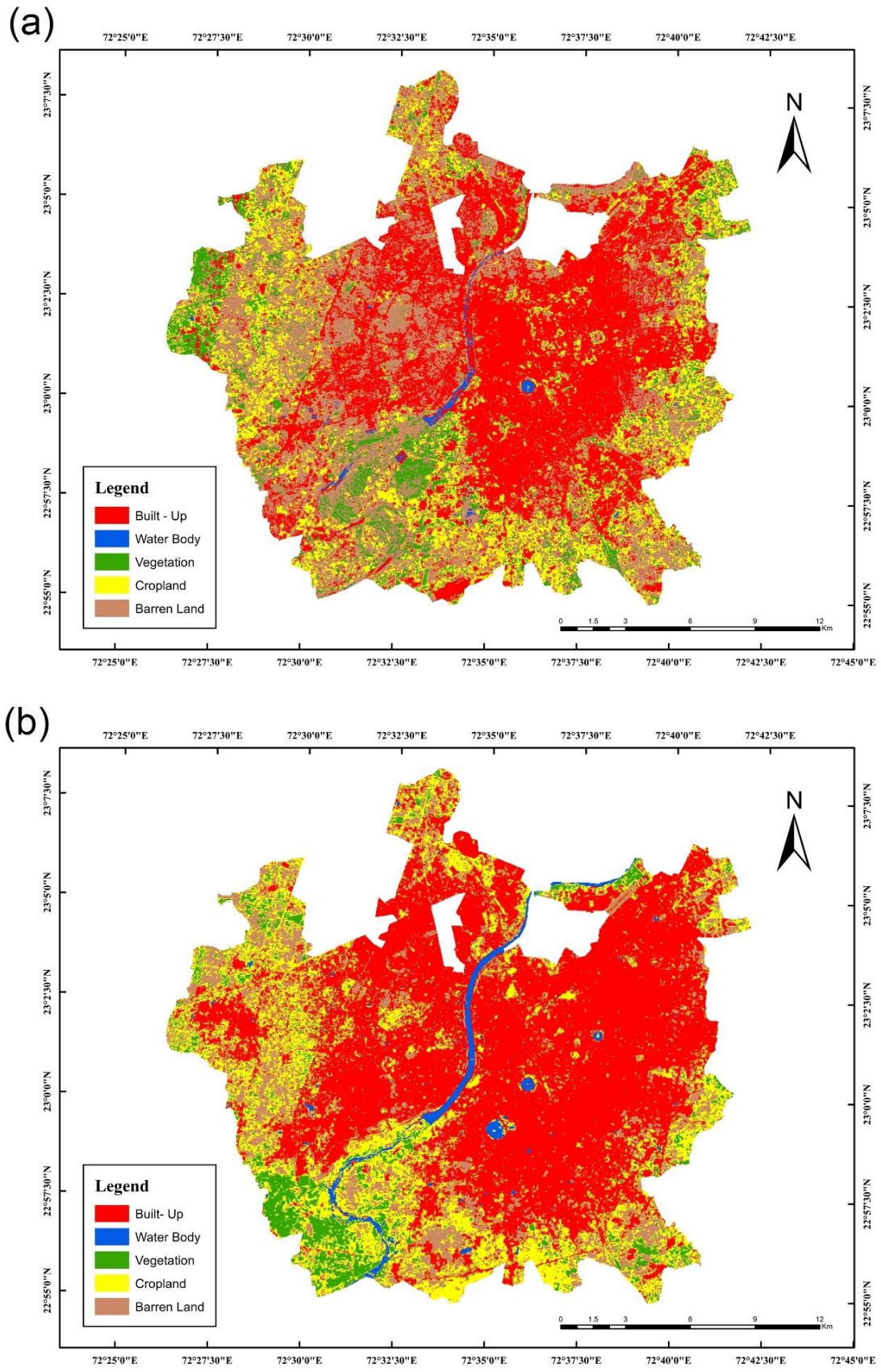

Figure 4 LULC Map of Ahmedabad for (a) 2000, (b) 2020.

Upon interpreting the results of the LULC classification, it can be noted that built-up areas exhibited the most pronounced growth during the study period, i.e., increasing from 161.40 km^2 in

2000 to 223.39 km^2 in 2020, with a net gain of 61.99 km^2. If we consider percentage values, this expansion has increased the proportion of built-up land from 40.18% to 55.60% during the study period. The pattern of growth in the city is basically outward expansion into peri-urban areas and densification of existing urban zones. Whereas the barren land decreased drastically from 125.72 km^2 to 50.84 km^2, showing a net loss of 74.88 km^2, and the net percentage share declined sharply from 31.29% to 12.65%, indicating a shift from open or barren spaces into mainly built-up and other land-use types.

The vegetation in the city also declined in the study period from 33.04 km^2 in 2000 to 22.19 km^2 in 2020, with a net loss of 10.85 km^2, and the share of vegetation class decreased from 8.22% to 5.52%, which shows a gradual decrease in the green spaces of the city. On the other hand, the cropland showed a different trend: it increased from 79.25 km^2 to 97.35 km^2, with a gain of 18.10 km^2 and a rise in its proportion from 19.73% to 24.23%, primarily observed in peri-urban areas. The water bodies, although covering only a small proportion of the total city area, increased from 2.33 km^2 in 2000 to 7.97 km^2 in 2020, showing a net gain of 5.64 km^2.

3.2 Accuracy Assessment

The accuracy level of LULC was evaluated using confusion matrices derived from independent validation samples. The detailed accuracy metrics used are presented in Table 5.

Table 5 Accuracy Assessment of LULC Maps.

Classes	**User Accuracy (%)**		**Producer Accuracy (%)**	
	2000	**2020**	**2000**	**2020**
Built-up	100.0	100.0	98.4	90.6
Water Body	100.0	100.0	100.0	100.0
Dense Vegetation	69.2	72.1	83.6	81.9
Cropland	70.5	74.3	90.1	86.8
Barren Land	65.1	60.8	98.2	68.3
	2000		**2020**	
Overall Accuracy	89.6%		93.2%	
Kappa Coefficient	84.2		86.7	

In 2000, the classification achieved an overall accuracy of 89.6% and a Kappa coefficient of 0.84, which shows a considerable level of accuracy between the classified and reference datasets, whereas in 2020, the classification accuracy had an overall accuracy of 93.2% and a Kappa coefficient of 0.86, which indicates a better classification of the satellite data. The user's accuracy for the Built-up and Water Body classes was 100% in both years, showing the highest accuracy for both classes. On the other hand, dense vegetation and cropland classes exhibited moderate user's Accuracy values ranging between 69% and 75%, while barren land showed comparatively lower user's accuracy due to similarities in the spectral signatures of the dry surface classes. The producer's accuracy remained high for Built-up and Water Body classes across both years, whereas barren land showed a decline in producer's accuracy from 98.2% in 2000 to 68.3% in 2020, possibly due to more classification confusion in the fringe areas owing to the spatial resolution of the city.

3.3 Land Surface Temperature Distribution

The spatial distribution of LST for Ahmedabad shows that the city's surface temperatures have increased markedly between 2000 and 2020 (Figure 5). In 2000, LST values ranged from 33.63°C to 38.97°C, which shows relatively moderate heat stress across the city, where higher temperatures were primarily confined to localized pockets in the western and south-western areas, while lower LST values were found in central and eastern zones in the areas with a lower built-up density and higher presence of vegetation.

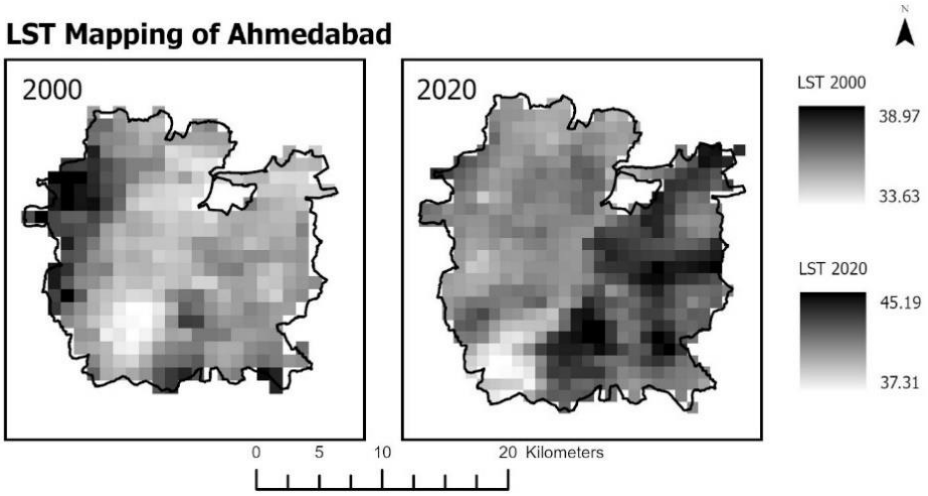

Figure 5 LST Mapping of Ahmedabad (in °C).

By 2020, the extent and intensity of high LST zones in the city increased, with minimum and maximum values rising to 37.31°C and 45.19°C, respectively, showing a rise of more than 6°C in the maximum surface temperature over the two-decade period (Figure 6). The high-temperature zones were more pronounced in the eastern and south-eastern areas, coinciding with dense built-up and industrial regions. In contrast, lower LST values were mainly limited to areas with water bodies and limited vegetation, indicating moderate thermal stress.

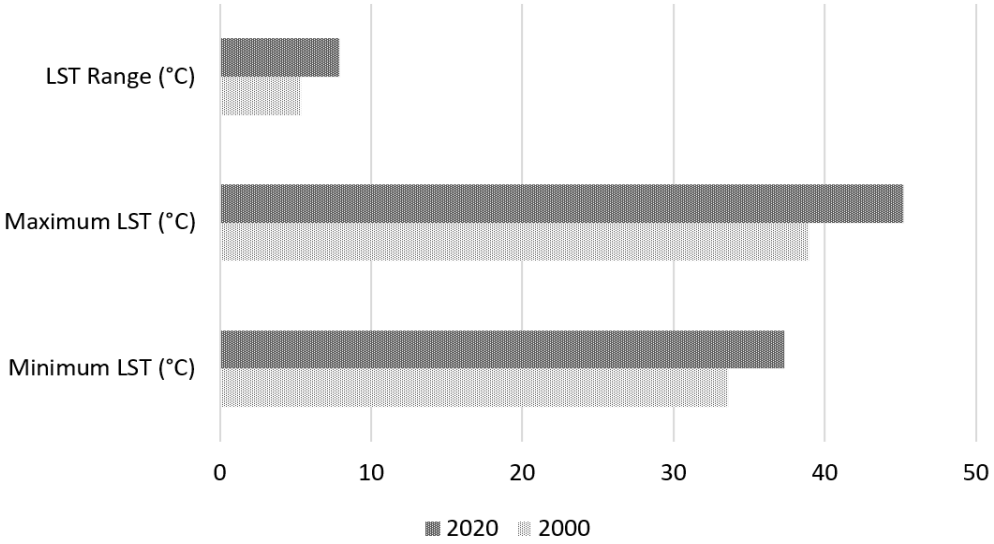

Figure 6 LST Extreme Values of Ahmedabad.

The increase in the LST range from 2000 to 2020 indicates greater in thermal heterogeneity across the city, highlighting the intensification of heat stress in Ahmedabad.

3.4 Urban Thermal Field Variance Index (UTFVI) Analysis

The UTFVI assessed patterns of thermal stress and how they have intensified and changed over the study period. The UTFVI maps for 2000 and 2020 (Figure 7) show a pronounced shift in the distribution and intensity of thermal stress across Ahmedabad. In 2000, most of the metropolitan area, especially the central and southern parts, had low thermal stress, showing balanced surface temperatures, whereas moderate stress zones appeared in mixed land-use areas, and the high stress was limited to small urban pockets in the west and southwest. This means that at the start of the study, thermal stress was focused in certain built-up areas and was not very spatially concentrated. By 2020, moderate and high thermal stress zones had expanded significantly, and high-stress areas became more pronounced and widespread. The high UTFVI values were mainly observed in eastern and south-eastern Ahmedabad, in areas with dense built-up and industrial development. The moderate thermal stress zones expanded across the city, indicating an increasing trend in thermal conditions. On the other hand, the low thermal stress zones became more fragmented and were largely confined to areas associated with water bodies and vegetated land. The comparative UTFVI analysis demonstrates that urban thermal stress in Ahmedabad has not only intensified but also expanded significantly over the past two decades. The transition from localised, highly stressed areas in 2000 to widespread moderate-to-high thermal-stress zones in 2020.

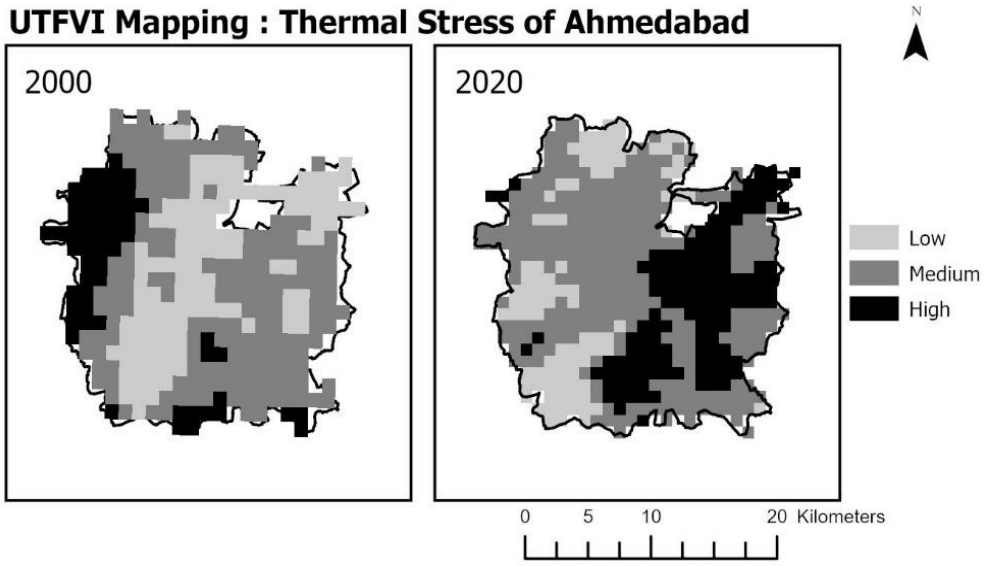

Figure 7 UTFVI Mapping and Thermal Stress Zones.

Upon calculating the area statistics for the latest 2020 UTFVI mapping, it was found that 35.53% of Ahmedabad city falls under the low thermal stress category, the moderate thermal stress category accounts for 50.92% of the total area, and around 13.55% of the total region is classified under high thermal stress. In the year 2020, high UTFVI zones were concentrated in the outskirts of industrial regions located in the eastern parts, like the Old City area, Khadia, and selected areas characterized by barren land, whereas low UTFVI zones were mainly distributed along the Sabarmati River corridor and around major water bodies (Table 6).

Table 6 Thermal Stress Locations for the year 2020.

City	High Thermal Stress	Low Thermal Stress
Ahmedabad	Industrial areas along the eastern parts of the city, Old City, Khadia, and some peri-urban areas in the form of barren land towards the south of the city	Areas along the Sabarmati River and a few peri-urban areas of the city, including around Kankaria Lake and Chandola Lake.

3.5 Predicted LULC Scenario for 2045

The future LULC changes were simulated using the ANN-based MOLUSCE model. The predicted spatial distribution of LULC classes is presented in Figure 8, while the projected area statistics are shown in Table 7.

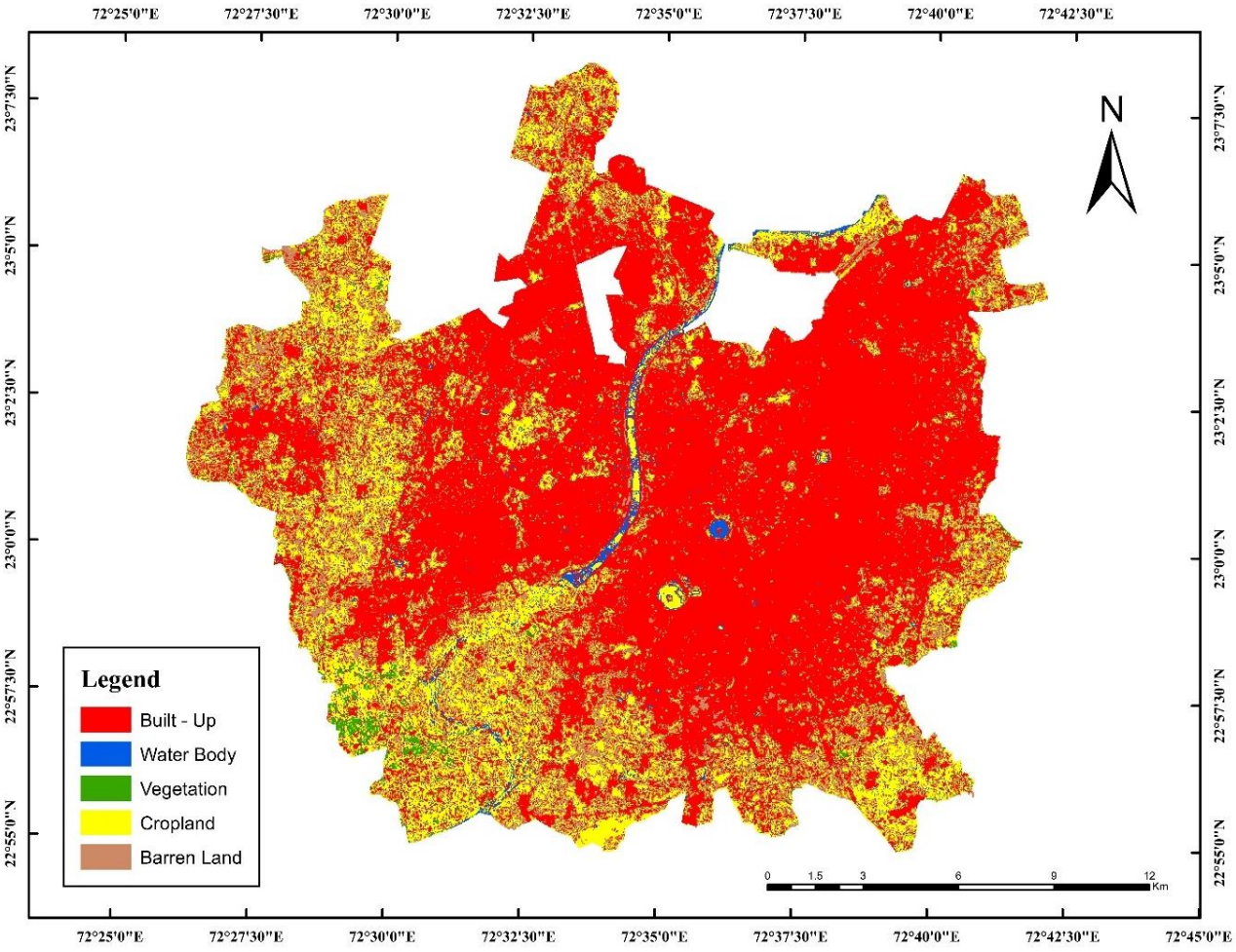

Figure 8 Simulated LULC of Ahmedabad for 2045.

Table 7 Area Statistics of LULC classes in the years 2000, 2020, and 2045.

LULC Class	2000 (km^2)	2020 (km^2)	2045 (km^2)	Percentage			Change (km^2) (2000-2020)	% Change (2000-2020)	Change (km^2) (2020-2045)	% Change (2020-2045)
				2000	2020	2045				
Built-Up	161.4	223.39	310.22	40.18	55.54	77.06	61.99	15.43%	86.56	21.52%
Waterbody	2.33	7.97	4.46	0.58	1.99	1.11	5.63	1.40%	-3.57	-0.88%
Vegetation	33.04	22.19	4.99	8.22	5.53	1.24	-10.84	-2.70%	-17.28	-4.29%
Cropland	79.25	97.35	57.35	19.73	24.27	14.25	18.11	4.51%	-40.39	-10.02%
Barren land	125.72	50.84	25.67	31.29	12.66	6.38	-74.88	-18.64%	-25.32	-6.28%

The simulation results indicate continued expansion of built-up areas, projected to reach 310.22 km^2 by 2045, a 92% increase from 2000. The vegetation cover is projected to decline sharply from 33.04 km^2 in 2000 to 4.99 km^2 in 2045, representing an 85% reduction. The barren land is expected to decrease from 125.72 km^2 to 25.67 km^2, and cropland from 97.35 km^2 in 2020 to 57.35 km^2 in 2045, which could put pressure on the existing barren and agricultural lands in the periphery of the city. The water bodies exhibit a non-linear trend, increasing between 2000 and 2020 but declining to 4.46 km^2 by 2045.

The temporal progression of area and percentage changes from 2000 to 2020 and 2045 is illustrated in Figure 9(a-d). These results show a dominant trend of urbanisation accompanied by the contraction of ecological and agricultural LULC classes.

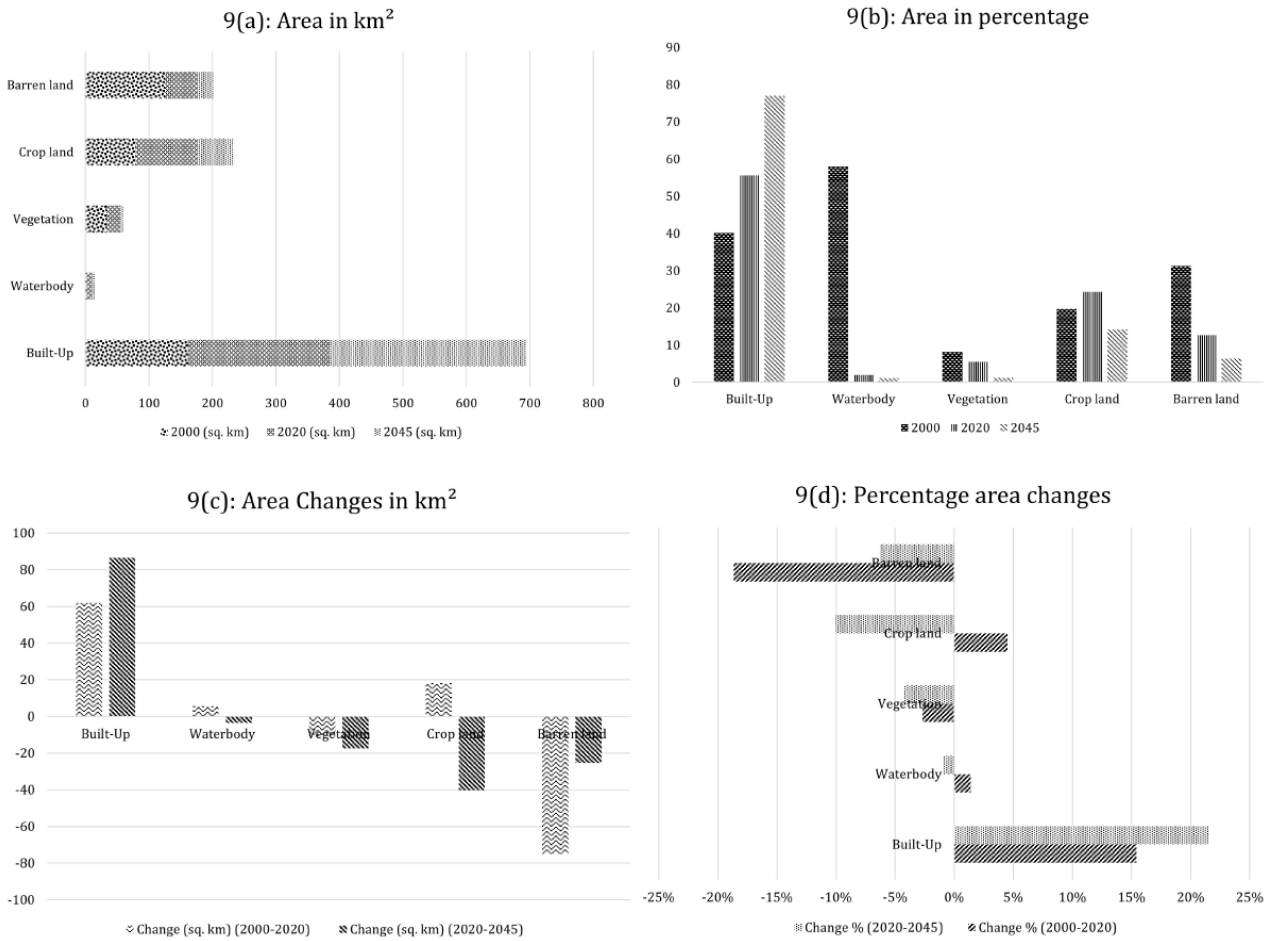

Figure 9 Findings for the year 2000, 2020, 2045. (a)Area in km^2; (b) Area in per cent; (c) Area Changes in km^2; (d) Per cent area change.

3.6 Transition Dynamics and ANN Model Performance

The ANN model implemented in the MOLUSCE framework was trained on historical LULC transitions and auxiliary variables. During ANN training, these parameters were set to effectively capture complex spatial transitions: 1000 iterations, 10 hidden layers, a learning rate of 0.1, a 1 × 1-pixel neighborhood, and a momentum of 0.05. The ANN parameters used in the simulation are summarised in Table 8.

Table 8 ANN Parameters for LULC Simulation in MOLUSCE.

Parameter	Value
Neighborhood	1 × 1 pixel
Learning Rate	0.100
Maximum Iterations	1000
Hidden Layers	10
Momentum	0.050

The model performance was tested using the Kappa Index of Agreement, which yielded values greater than 0.85, which strongly supports agreement between simulated and observed existing

LULC. The improvement in classification accuracy between 2000 and 2020 contributed to the robustness of the predictive simulation. The simulated 2045 LULC map represents a plausible future LULC scenario for the city, providing a spatially explicit basis for assessing potential land transformation trends in Ahmedabad.

4. Discussion

The integrated analysis of LULC, LST, UTFVI, and future land-use simulations provides a comprehensive understanding of how urban ecological systems have evolved and of their future scenarios for Ahmedabad. The results collectively reveal that rapid urban expansion has not only altered the city's biophysical characteristics but also significantly changed the thermal environment, which has increased climate-related risks.

4.1 LULC and Thermal Environment

The significant increase in built-up land between 2000 and 2020 relates to Ahmedabad's rapid urban expansion along major infrastructure and industrial corridors. Significant urban growth is evident in the eastern and southeastern zones, which include the areas around Vatva, Naroda, Odhav, and Aslali, all of which have established industrial estates. These zones have experienced the sustained conversion of barren and agricultural land into manufacturing units, warehouses, and worker housing, thereby contributing to the formation of dense, impervious urban surfaces. The areas of western Ahmedabad, particularly Bopal, Ghuma, Shela, and South Bopal, have witnessed large-scale residential and commercial development, driven by real estate expansion, improved road connectivity, and increased proximity to educational and institutional hubs. Similarly, in the northern periphery, including Chandkheda and Motera, have expanded rapidly due to the development of transport infrastructure and several urban amenities. These spatial trends are consistent with the observed decline in barren land and vegetation in the LULC analysis, as open lands in the fringe areas have been largely absorbed into the city fabric. The large-scale development initiatives by the government, such as the Gujarat International Finance Tec-City (GIFT City) near Gandhinagar, the Delhi-Mumbai Industrial Corridor (DMIC), and smart city-related investments, have accelerated LULC changes by improving regional accessibility and economic attractiveness.

4.2 LULC-LST Relationship and Spatial Thermal Patterns

The spatial distribution of LST shows a strong correspondence with the built-up morphology and land-cover composition of Ahmedabad. The persistently elevated LST values were mainly observed in the densely urbanised and industrial zones, including Vatva GIDC, Naroda GIDC, Odhav, and the historic city core encompassing Kalupur, Khadia, and Manek Chowk. The high building density, impervious surfaces, narrow streets, and limited vegetation cover are the visible characteristics of these areas of high LST. The dominance of concrete and asphalt surfaces in these zones increases absorption of solar radiation and heat retention, contributing to elevated LST and reduced nighttime cooling. On the other hand, lower LST values were found mainly along the Sabarmati River corridor, particularly in areas influenced by the Sabarmati Riverfront Development Project, as well as around major urban water bodies. The presence of open water surfaces, riparian zones, and landscaped

green spaces in these areas increases evaporative cooling and moderates surface temperatures. This pronounced contrast between the high-temperature built-up zones and cooler blue-green landscapes indicates the crucial role of land-cover heterogeneity and urban green-blue infrastructure in regulating surface thermal conditions in cities.

4.3 UTFVI Patterns and Urban Heat Stress Hotspots

The UTFVI analysis provides an accurate assessment of urban heat stress by normalizing LST variations relative to the citywide thermal characteristics. The high-UTFVI zones were predominantly found in industrial clusters and high-density residential areas, particularly in eastern Ahmedabad and parts of the historic urban core. These locations are typically characterised by limited green cover, greater human-generated heat emissions, aging infrastructure, and urban infrastructure that is often not designed to be climate-responsive. The moderate UTFVI zones are quite extensive and dominate the peri-urban areas undergoing rapid land conversion along Sanand Road, Sarkhej, and the peripheral zones near Changodar. These areas are generally characterised by mixed land-use and represent critical transition zones where future development patterns could substantially influence thermal conditions. Whereas, the low-UTFVI zones were primarily found along riverine landscapes, green campuses, and existing peri-urban agricultural areas. The strong links between high-UTFVI zones and areas of dense built-up concentration highlight the cumulative influence of land-use transformation on urban heat stress; rather than reflecting isolated temperature anomalies, the observed UTFVI patterns demonstrate a systemic intensification of thermal stress across the city.

The projected LULC scenario for 2045 indicates a continued expansion of built-up land across Ahmedabad's city limits, particularly along new growth corridors connecting Ahmedabad to Sanand, Changodar, and Gandhinagar. If these predicted trends come to pass, the future urban landscape will be dominated by impervious surfaces, with reduced vegetation and agricultural land.

Given the strong empirical association between built-up density and elevated LST observed in the temporal analysis, it is reasonable to predict that urban heat stress is subject to intensification. The areas currently classified as moderate UTFVI zones, especially peri-urban growth fronts, are likely to transform into high thermal stress zones as vegetation will be replaced by urban infrastructure. The projected reduction in vegetation and water bodies further suggests a weakening of natural cooling mechanisms, increasing the likelihood of extreme surface temperatures during the summer season.

5. Conclusion

This study provides a comprehensive overview of LULC, thermal characteristics, and future LULC trajectories in the city of Ahmedabad by integrating remote sensing tools, machine-learning-based classification, thermal indicators, and predictive modelling. The results of the study indicate that rapid urban expansion between 2000 and 2020 has significantly modified Ahmedabad's LULC, with built-up areas expanding significantly due to declines in barren land, vegetation, and agricultural areas. This transformation is most visible along major growth corridors and industrial zones, such as Vatva, Naroda, Odhav, and the western peri-urban belt, including Bopal and South Bopal, which reflect the combined effects of infrastructure development, industrialisation, and real estate-driven expansion.

The multi-temporal LST analysis for 2000 and 2020 shows that areas characterised by dense built-up surfaces and industrial activity have consistently experienced increases in LST values in both years, and that high-temperature zones have expanded and intensified by 2020. Areas influenced by water bodies and vegetation, like the Sabarmati River corridor, Kankaria Lake, and Chandola Lake, have maintained comparatively lower thermal characteristics. However, the total area of these thermally moderate zones has reduced over time. The UTFVI-based assessment proves that a significant portion of the city has moved from lower to moderate and high thermal stress zones between 2000 and 2020, especially in eastern industrial zones and the historic city core.

The future LULC simulation for 2045 indicates a growing trend in the city, with built-up areas simulated to dominate the urban fabric. Further, it may encroach upon remaining vegetation, cropland, and open spaces. The observed increase in LST over the decade, the corresponding increases in high UTFVI, and the projected LULC scenario suggest a possible intensification of thermal stress in the absence of specific policy intervention. The peri-urban areas, especially those connecting Ahmedabad with Sanand, Changodar, and Gandhinagar, are more vulnerable, as areas currently experiencing moderate thermal stress may change into high-stress zones. The projected trajectories are consistent with findings from other rapidly urbanising cities in India, such as Delhi, Surat, and Hyderabad, as well as with global studies that highlight the long-term effects of uncontrolled urban expansion.

This integrated framework in the study provides valuable information, but a few limitations persist, such as the use of moderate-resolution MODIS LST data, which may be suitable for a multi-temporal regional-scale assessment of LST, but it may not fully capture micro-scale thermal variations in highly diverse urban areas. The future land-use simulation assumes the continuation of historical trends and does not incorporate the city's social and economic aspects. The study focused on thermal variability in the city's summer months and did not conduct a multi-season analysis. Future research can address these limitations by using higher-resolution thermal data and socio-economic variables to enhance urban heat risk assessment.

Despite these limitations, the results underscore the growing importance of integrating land-use planning with climate-sensitive urban development policies. The increase in LST and expansion of thermal stress zones between 2000 and 2020 highlight the urgency of preserving and enhancing blue green infrastructure of the cities by protecting the remaining agriculture and open spaces specifically including climate responsive building design, strict enforcement land use zoning regulations, and considering thermal aspects into all the development projects by private as well as public sector to improve resilience for the residents to combat against the climate change in the cities.

Author Contributions

R.K.G. developed the initial concept for this article and provided comprehensive editing and oversight throughout the process. Y.K.T. was responsible for curating the data analysis and ensuring accuracy and relevance. G.Y. & A.G. prepared the initial draft and executed the necessary computations while validating the analytical methods employed in this research. S.G. explored specific approaches and oversaw the interpretation of the findings presented in the study.

Competing Interests

The authors have declared that no competing interests exist.

AI-Assisted Technologies Statement

The authors used AI-assisted tools (Grammarly) only for language refinement and editorial support. All scientific analysis, interpretation, and conclusions are solely the responsibility of the authors.

References

1. Mauree D, Naboni E, Coccolo S, Perera AT, Nik VM, Scartezzini JL. A review of assessment methods for the urban environment and its energy sustainability to guarantee climate adaptation of future cities. Renew Sustain Energy Rev. 2019; 112: 733-746.
2. Mamun AA, Mahmood A, Rahman M. Identification and monitoring the change of land use pattern using remote sensing and GIS: A case study of Dhaka City. IOSR J Mech Civil Eng. 2013; 6: 20-28.
3. Bhatta B. Measurement and analysis of urban growth. In: Analysis of urban growth and sprawl from remote sensing data. Berlin, Heidelberg: Springer Berlin Heidelberg; 2010. pp. 85-106.
4. Baqa MF, Chen F, Lu L, Qureshi S, Tariq A, Wang S, et al. Monitoring and modeling the patterns and trends of urban growth using urban sprawl matrix and CA-Markov model: A case study of Karachi, Pakistan. Land. 2021; 10: 700.
5. Subedi P, Subedi K, Thapa B. Application of a hybrid cellular automaton-Markov (CA-Markov) model in land-use change prediction: A case study of Saddle Creek Drainage Basin, Florida. Appl Ecol Environ Sci. 2013; 1: 126-132.
6. AbdelRahman MA, Natarajan A, Hegde R, Prakash SS. Assessment of land degradation using comprehensive geostatistical approach and remote sensing data in GIS-model builder. Egypt J Remote Sens Space Sci. 2019; 22: 323-334.
7. Singh S, Srivastava R. Impact of land use changes on water resource: Assessment through remote sensing and geographical information systems (GIS). In: Advances in water resource planning and sustainability. Singapore: Springer Nature Singapore; 2023. pp. 169-181.
8. Mfwango LH, Kisiki CP, Ayenew T, Mahoo HF. The impact of land use/cover change on surface runoff at Kibungo sub-catchment of Upper Ruvu catchment in Tanzania. Environ Chall. 2022; 7: 100466.
9. Batar AK, Watanabe T, Kumar A. Assessment of land-use/land-cover change and forest fragmentation in the Garhwal Himalayan Region of India. Environments. 2017; 4: 34.
10. Lambin EF, Meyfroidt P. Global land use change, economic globalization, and the looming land scarcity. Proc Natl Acad Sci U S A. 2011; 108: 3465-3472.
11. Faruque MJ, Vekerdy Z, Hasan MY, Islam KZ, Young B, Ahmed MT, et al. Monitoring of land use and land cover changes by using remote sensing and GIS techniques at human-induced mangrove forests areas in Bangladesh. Remote Sens Appl. 2022; 25: 100699.
12. Kotowska D, Báldi A, Dobosy P, Felföldi T, Garamszegi LZ, Horváth Z, et al. Aligning land use with sustainability: Context-sensitive pathways forward. J Environ Manage. 2025; 394: 127252.

13. Kafi KM, Shafri HZ, Shariff AB. An analysis of LULC change detection using remotely sensed data; A Case study of Bauchi City. IOP Conf Ser Earth Environ Sci. 2014; 20: 012056.
14. Forkuo EK, Biney E, Harris E, Quaye-Ballard JA. The impact of land use and land cover changes on socioeconomic factors and livelihood in the Atwima Nwabiagya district of the Ashanti region, Ghana. Environ Chall. 2021; 5: 100226.
15. Wakode HB, Baier K, Jha R, Azzam R. Analysis of urban growth using Landsat TM/ETM data and GIS—A case study of Hyderabad, India. Arab J Geosci. 2014; 7: 109-121.
16. Zhang C, Sargent I, Pan X, Li H, Gardiner A, Hare J, et al. An object-based convolutional neural network (OCNN) for urban land use classification. Remote Sens Environ. 2018; 216: 57-70.
17. Verburg PH, Soepboer W, Veldkamp A, Limpiada R, Espaldon V, Mastura SS. Modeling the spatial dynamics of regional land use: The CLUE-S model. Environ Manage. 2002; 30: 391-405.
18. Sudhira HS, Ramachandra TV, Jagadish KS. Urban sprawl: Metrics, dynamics and modelling using GIS. Int J Appl Earth Obs Geoinf. 2004; 5: 29-39.
19. Bag A, Sharma A, Pal S. Studying urbanization pattern in Sambalpur City during 1992-2042 using CA-ANN, and Markov-Chain model. Int J Eng Geosci. 2024; 9: 356-367.
20. Ambreen H, Rahman AU. Evaluating spatio-temporal dynamics in LULC and its implications on land surface temperature of Swat valley, Eastern Hindukush. Int J Eng Geosci. 2025; 10: 495-503.
21. Devkota P, Dhakal S, Shrestha S, Shrestha UB. Land use land cover changes in the major cities of Nepal from 1990 to 2020. Environ Sustain Indic. 2023; 17: 100227.
22. Sharma GK, Ghuge VV. Spatio-temporal analysis of urban growth in the Mumbai metropolitan area using Landsat imagery. Discov Cities. 2025; 2: 100.
23. Rahman MM, Szabó G. Impact of land use and land cover changes on urban ecosystem service value in Dhaka, Bangladesh. Land. 2021; 10: 793.
24. Gupta RK. Identifying urban hotspots and cold spots in Delhi using the Biophysical Landscape framework. Ecol Econ Soc. 2024; 7: 137-155.
25. Üstün Topal T. Evaluation of the relationship between spatial-temporal changes of land use/land cover (LULC) and land surface temperature (LST): A case study of Nilüfer, Bursa. Turkiye Peyzaj Arast Derg. 2023; 6: 56-74.
26. Gupta R. GIS-based analysis of land surface characteristics and urban heat islands in metropolitan cities of India. Int J Eng Geosci. 2025; 10: 440-455.
27. Mishra A, Arya DS. Assessment of land-use land-cover dynamics and urban heat island effect of Dehradun city, North India: A remote sensing approach. Environ Dev Sustain. 2024; 26: 22421-22447.
28. Morsy S, Hadı M. Impact of land use/land cover on land surface temperature and its relationship with spectral indices in Dakahlia Governorate, Egypt. Int J Eng Geosci. 2022; 7: 272-282.
29. Taha H. Urban climates and heat islands: Albedo, evapotranspiration, and anthropogenic heat. Energy Build. 1997; 25: 99-103.
30. Ahmad MN, Shao Z, Javed A, Ahmad I, Islam F, Skilodimou HD, et al. Optical-SAR data fusion based on simple layer stacking and the XGBoost algorithm to extract urban impervious surfaces in global alpha cities. Remote Sens. 2024; 16: 873.
31. Jat MK, Garg PK, Khare D. Monitoring and modelling of urban sprawl using remote sensing and GIS techniques. Int J Appl Earth Obs Geoinf. 2008; 10: 26-43.

32. Rawat JS, Kumar M. Monitoring land use/cover change using remote sensing and GIS techniques: A case study of Hawalbagh block, district Almora, Uttarakhand, India. Egypt J Remote Sens Space Sci. 2015; 18: 77-84.
33. Seto KC, Güneralp B, Hutyra LR. Global forecasts of urban expansion to 2030 and direct impacts on biodiversity and carbon pools. Proc Natl Acad Sci. 2012; 109: 16083-16088.
34. Alavipanah S, Wegmann M, Qureshi S, Weng Q, Koellner T. The role of vegetation in mitigating urban land surface temperatures: A case study of Munich, Germany during the warm season. Sustainability. 2015; 7: 4689-4706.
35. Zhou W, Pickett ST, Cadenasso ML. Shifting concepts of urban spatial heterogeneity and their implications for sustainability. Landsc Ecol. 2017; 32: 15-30.
36. Mohan M, Kikegawa Y, Gurjar BR, Bhati S, Kolli NR. Assessment of urban heat island effect for different land use–land cover from micrometeorological measurements and remote sensing data for megacity Delhi. Theor Appl Climatol. 2013; 112: 647-658.
37. Aqdas M, Usmani TM, Benhizia R, Szabó G. Urban expansion and thermal stress: A remote sensing analysis of LULC and urban heat islands in Ghaziabad, India. Land. 2025; 14: 1893.
38. Mahata B, Sahu SS, Sardar A, Laxmikanta R, Maity M. Spatiotemporal dynamics of land use/land cover (LULC) changes and its impact on land surface temperature: A case study in New Town Kolkata, eastern India. Reg Sustain. 2024; 5: 100138.
39. Kavathekar V, Tripathy AK, Chettri SK, Bhanage V. Evaluation of land use land cover dynamics and urban heat island effects over Mumbai metropolitan Region, India. Int J Environ Sci Technol. 2025; 22: 11345-11368.
40. Dapke P, Quadri SA, Nagare SM, Bandal SB, Baheti MR. A Comparative analysis machine learning techniques for LULC classification using landsat-8 satellite imagery. Int J Eng Geosci. 2025; 10: 84-92.
41. Zhu XX, Tuia D, Mou L, Xia GS, Zhang L, Xu F, et al. Deep learning in remote sensing: A comprehensive review and list of resources. IEEE Geosci Remote Sens Mag. 2017; 5: 8-36.
42. Saharan D, Nehra S. Geospatial assessment and prediction of land use changes in Bikaner Urbanizable area: A QGIS-based approach using MOLUSCE plugin. Int J Environ Sci. 2025; 11: 130-142.
43. Blissag B, Yebdri D, Kessar C. Spatiotemporal change analysis of LULC using remote sensing and CA-ANN approach in the Hodna basin, NE of Algeria. Phys Chem Earth. 2024; 133: 103535.
44. Dewan AM, Yamaguchi Y. Land use and land cover change in Greater Dhaka, Bangladesh: Using remote sensing to promote sustainable urbanization. Appl Geogr. 2009; 29: 390-401.
45. Mohan M, Pathan SK, Narendrareddy K, Kandya A, Pandey S. Dynamics of urbanization and its impact on land-use/land-cover: A case study of megacity Delhi. J Environ Prot. 2011; 2: 1274-1283.
46. Li X, Zhou Y, Zhu Z, Liang L, Yu B, Cao W. Mapping annual urban dynamics (1985-2015) using time series of Landsat data. Remote Sens Environ. 2018; 216: 674-683.
47. Rwanga SS, Ndambuki JM. Accuracy assessment of land use/land cover classification using remote sensing and GIS. Int J Geosci. 2017; 8: 611-622.
48. Gupta A, Gupta RK, Yadav G, Mandal NG. The effects of vegetation & bare land on thermal characteristics: A case study of three Indian metropolitan areas. Res Ecol. 2025; 7: 1-19.

49. Vasanthawada SR, Puppala H, Prasad PR. Assessing impact of land-use changes on land surface temperature and modelling future scenarios of Surat, India. Int J Environ Sci Technol. 2023; 20: 7657-7670.
50. Assaf G, Assaad RH. Modeling the impact of land use/land cover (LULC) factors on diurnal and nocturnal Urban Heat Island (UHI) intensities using spatial regression models. Urban Clim. 2024; 55: 101971.
51. Chatterjee U, Majumdar S. Impact of land use change and rapid urbanization on urban heat island in Kolkata city: A remote sensing based perspective. J Urban Manage. 2022; 11: 59-71.
52. Ahmad MN, Almutlaq F, Huq ME, Islam F, Javed A, Skilodimou HD, et al. Enhanced urban impervious surface land use mapping using a novel multi-sensor feature fusion method and remote sensing data. Environ Earth Sci. 2025; 84: 228.